Solid-State Electronics Vol. 35, No. 3, pp. 239–250, 1992
Printed in Great Britain.

0038-1101/92 $5.00 + 0.00

INVITED PAPER

MEASUREMENT OF MINORITY-CARRIER LIFETIME BY TIME-RESOLVED PHOTOLUMINESCENCE

R. K. AHRENKIEL
National Renewable Energy Laboratory, 1617 Cole Boulevard, Golden, CO 80401, U.S.A.

(Received 30 July 1991; in revised form 23 September 1991)

Abstract—Much of the current compound semiconductor device research is based on minority-carrier devices such as heterojunction bipolar transistors and diode lasers. The improvement of minority-carrier-parameters is the focal point of much ongoing materials research. The minority-carrier lifetimes of III–V compound semiconductors are most easily characterized by time-resolved photoluminescence. This is a quick and contactless technique which directly measures the excess minority-carrier carrier density. By using a focused laser beam as the excitation source, the required sample area may be very small. In special diagnostic structures which utilize a confinement or passivating layer, the interface recombination velocity can be determined. Here I will describe the measurement theory and measurement techniques which are used in our laboratory. Recent developments in the III–V materials technology will be reviewed.

INTRODUCTION

The minority-carrier lifetime is a very important parameter for a wide range of minority-carrier devices. There have been several recent publications describing general methods for the measurement of minority-carrier lifetime in semiconductors. Two recent textbooks have provided descriptions of a variety of minority-carrier lifetime measurement[1,2] techniques. The measurement of minority-carrier lifetime in compound semiconductors is usually performed by a time-resolved photoluminescence technique[1] (TRPL). The specific TRPL technique used in our laboratory is called time-resolved single photon counting. This is a nondestructive and noninvasive measurement which is very time-efficient[3,4]. For process control and evaluation, one can measure lifetime in a simple structure rather than fabricating a complete device and evaluating its performance. The individual components or epilayers can often be separately optically probed in the procedures to be described.

This paper will be largely limited to lifetime studies on GaAs and the standard window/passivating epitaxial layer composed of various $Al_xGa_{1-x}As$ compositions. GaAs Is an excellent case study which will be used to illustrate the experimental techniques and analysis methods. An extensive review[5] of lifetime data of other III–V materials was recently published.

Here I will focus on the diagnostic measurements performed at the Solar Energy Research Institute (SERI) over the last several years. This facility current produces many lifetime measurements per year in collaboration with numerous U.S. and foreign research groups. This research encompasses both process development and basic research using TRPL as the measurement technique. Use of the data from these measurements has also been useful for predicting and improving device performance. An example is that the TRPL diagnostic was used in colloboration with two materials research groups to produce the largest reported lifetime for undoped and moderately doped ($1 \times 10^{17}\,cm^{-3}$) epitaxial GaAs, respectively. Here, recent innovations and improvements in the technology will be emphasized.

BACKGROUND

The development of the III–V materials technology has accelerated in the last decade in parallel with the wide variety of III–V devices. Complementary device research has focused on heterojunction bipolar transistors, lasers, light-emitting diodes (LEDs) and photovoltaic devices. All of the above devices are based on minority-carrier transport and maximizing the minority-carrier lifetime and minimizing interface recombination velocity are crucial components of materials research. Current device research is focused primarily on III–V epitaxial materials rather than bulk crystals.

As will be shown here, the TRPL technique is a quick, direct and contactless measurement of the excess minority-carrier concentration as a function of time. The transient decay of the photoluminescence signal is called the photoluminescence lifetime and may be less than the true minority-carrier lifetime. When combined with a model of the transient response, which is derived from the diffusion equation, the minority-carrier lifetime and other recombination lifetimes are calculated. The analysis of a common

diagnostic structure, the isotype double heterostructure, will be discussed in a later section.

The earlier references describe a number of techniques for measurement of minority-carrier lifetime. Comprehensive reviews are given in Chap. 8 of the book by Schroder[1] and Chaps 3–6 of the work by Orton and Blood[2]. Other lifetime measurement methods include photoconductive decay, current or voltage decay, modulation methods, and others. Most of these measurements require diagnostic devices with ohmic contacts and are therefore somewhat more laborious to fabricate. Many of the measurements are less directly linked to the excess minority-carrier denisty and therefore require somewhat complicated parameter fits to the data. The phase shift technique is a contacless optical measurement of PL lifetime. This subject was recently reviewed by the author[5] and limitations discussed. The phase shift method was initially used in our laboratory but was replaced by TRPL. We found that TRPL data are easier to analyze and contain much additional information. In particular, the phase shift analysis assumes a pure exponential decay of the PL signal and may produce very misleading results if the decay is nonexponential. Checking the injection level by the phase shift technique is laborious. The nonexponential bimolecular decay[5], indicative of high injection, is observed directly in TRPL. It will be shown here that the excess minority-carrier decay is often nonexponential for other reasons and detailed features provide information about the specific recombination mechanisms.

EXPERIMENTAL TECHNIQUE

Most semiconducting materials emit near bandgap recombination radiation or photoluminescence (PL) upon photoexcitation with an appropriate light source. The technique is most useful for materials such as GaAs which are strong light emitters. In this case, TRPL is very sensitive and a wide range of recombination rates vs minority-carrier injection levels can be analyzed. Our technique uses high-speed electronics and photon counting to resolve PL decay times as small as 30 ps. Application of models, which are derived from solving the time-dependent diffusion equation for the device structure, also provide the determination of surface and interface recombination velocities.

When measuring the TRPL, one monitors the excess minority-carrier density as a function of time. The excess minority-carrier density is a function of both minority-carrier lifetime and the diffusion rate out of the acive region. Consequently, the excess minority-carrier density is structure dependent upon recombination and diffusion. An example[6] of the latter effect is the PL lifetime in surface passivated p–n junctions. Here the PL lifetime is a function of minority-carrier lifetime, diffusivity and device geometry, and is always less than the bulk lifetime. For the most accurate analysis of material lifetime, one can make special confinement devices which eliminate diffusion effects.

In this paper, the recombination mechanisms, which determine the lifetime in semiconducting materials, will be addressed. I will present recent data on the state-of-the-art epitaxial GaAs and $Al_xGa_{1-x}As$/GaAs interfaces. Some examples of the use of TRPL as a process development diagnostic will be presented. Data will show that the recombination velocity (S) of the $Al_xGa_{1-x}As$/GaAs interface is very dependent upon the growth temperature for certain epitaxial growth techniques. In addition, I will show some remarkable recent data on the use of epitaxial $Ga_{0.5}In_{0.5}P$ as an alternative passivating window layer for GaAs. Some experiments which measure the photon recycling effect in device structures will be discussed. Finally, data will be shown which indicate that the effective lifetime is dependent on the injection level when Shockley–Read–Hall recombination is dominant.

Our preferred technique for measuring TRPL is called time-correlated single-photon counting[7,8]. The experimental technique is currently most applicable to the larger bandgap materials with $E_g > 1.1$ eV. In order to use time-correlated single photon counting, the photodetector must be able to detect single photons produced by band-to-band recombination luminescence. The two commercial photodetectors with sufficient sensitivity for photon counting are photomultiplier tubes (PMT) and microchannel plates (MCP). Our apparatus uses a pulsed-dye laser to excite the PL in the device under test (DUT). The photodetector is followed by a high-speed amplifier which is connected to the photon-counting apparatus. A schematic of the experimental set-up is shown in Fig. 1. The photons emitted by the sample are focused on the input slit of a scanning monochromator. The latter is tuned to the appropriate wavelength which is that corresponding to the band-to-band recombination.

Our laboratory has two such measurement systems which are identical except for the photodetector. The original system uses an S-1 photomultiplier tube which has an impulse response of about 300 ps. The relatively long impulse response is caused by the transit time-dispersion of electrons as they cascade down the dynode chain. Transit time dispersion is greatly reduced with a newer detector called a microchannel plate detector. A newer system uses a Hamamatsu model R2809U microchannel plate detector which has a time resolution of 30 ps at full-width-at-half-maximum (FWHM). The time-correlated photon counting electronics are identical in the remainder of the detection system. Using a beam splitter and a photodiode, a small fraction of the laser light pulse is deflected to a fast photodiode. The electrical output of the photodiode triggers the time-to-amplitude converter (TAC). The pulse-height discriminator is necessary to block electrical pulses

which are produced by thermal and other nonphotonic sources. The PL photon first collected initiates an electrical pulse in the photodetector which is passed by the amplitude discriminator. The electrical pulse produces a stop message at the TAC. The TAC output is a ramp generator with an amplitude proportional to the time delay between the laser pulse and the arrival of the first photon. The TAC signal is fed to a multichannel pulse height analyzer (MCA) which collects one count per detected photon. A count is stored in a channel appropriate to the time delay and a maximum of one count is recorded for every laser pulse. In this way, a histogram of the PL decay is built up in terms of counts vs time.

RECOMBINATION MECHANISMS

The recombination mechanisms III–V materials can be described by three basic processes. These are raditive recombination, Shockley–Read–Hall[9–11] and Auger recombination. The radiative recombination rate R_r of free electrons and holes is given by[12]:

$$R_r = Bpn. \tag{1}$$

Here R is the recombination rate $\mathrm{cm}^{-3}\,\mathrm{s}^{-1}$ and p and n are the free hole and electron concentrations, respectively. The B-coefficient is specific to a particular semiconductor and is proportional to the dipole matrix elements between the conduction and valence-band wavefunctions. Therefore, B is much larger for direct than for indirect bandgap materials. For example, B is about $2 \times 10\,\mathrm{cm}^3\,\mathrm{s}^{-1}$ for GaAs[13,14] and about $1 \times 10^{-15}\,\mathrm{cm}^3\,\mathrm{s}^{-1}$ for Si at 300 K. One may easily show that the low-injection radiative lifetime is:

$$\tau_r = 1/(BN), \tag{2}$$

where N is the majority-carrier density.

The second important mechanism in minority-carrier kinetics is the Shockley–Read–Hall (SRH) nonradiative recombination mechanism. The SRH process is related to the presence of defects which produce quantum levels in the bandgap of the semiconductor. The derivation of the SRH recombination rate is given in most semiconductor textbooks[15] and is shown to be:

$$R = \frac{\sigma_p \sigma_n v_{th} N_t [pn - n_i^2]}{\sigma_n [n + n_i \exp(E_t - E_i/kT)] + \sigma_p [p + n_i \exp(E_i - E_t/kT)]}. \tag{3}$$

Here N_t is the density of deep levels, σ_p, σ_n are the hole, electron capture cross sections, respectively, and E_t is the energy level of the trap. The electron and hole concentrations are n and p, respectively, and v_{th} is the thermal velocity of the electron or hole.

The low-injection SRH recombination rate per excess minority-carrier for a defect level near the center of the bandgap ($E_t \sim E_i$) is given by:

$$R_{SRH} = \sigma v_{th} N_t = 1/\tau_{SRH}. \tag{4}$$

Here σ is the capture cross-section for the case $\sigma_n = \sigma_p$ and N_t is the volume density of defect centers. If there are a number of different recombination centers, the SRH lifetime is then given by:

$$\frac{1}{\tau\ \mathrm{SRH}} = v_{th} \sum_i (\sigma_i N_i). \tag{5}$$

Here σ_i and N_i are the capture cross-section and the volume density of the ith type of defect center.

The nonradiative centers that exist at surfaces or interfaces are often called interface states. A solution of the 2-D recombination problem at the interfacial plane is solved in terms of an interface recombination velocity $S(\mathrm{cm\,s}^{-1})$.

$$S = \sigma v_{th} N_s \tag{6}$$

where N_s is the planar density of recombination centers.

The Auger recombination mechanism involves the transfer of the electron–hole energy to a majority-carrier. The Auger[16] recombination lifetime may be shown to be:

$$\frac{t}{\tau_A} = \sigma_A N^2. \tag{7}$$

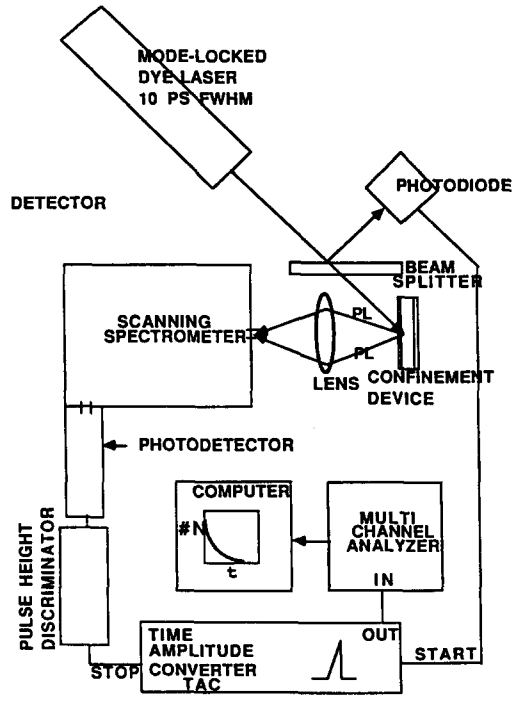

Fig. 1. Schematic of the measurement apparatus.

Here N is the majority-carrier density and σ_A is the Auger cross-section. One may get the total *bulk lifetime* by adding the recombination rates from the different mechanisms. The result is:

$$\frac{1}{\tau_B} = BN + \frac{1}{\tau_{SRH}} + \frac{t}{\tau_A}. \tag{8}$$

Very little data exist for TRPL measurements on GaAs at higher doping levels where Auger recombination may be the dominant mechanism. Very early data[17] on n-type GaAs wafers indicated a $1/N^2$ decrease in lifetime for $N > 2 \times 10^{18}\,\mathrm{cm}^{-3}$. The Auger effect in heavily-doped GaAs was discussed[18] in a recent review.

If the active region is free of nonradiative recombination centers and Auger recombination is not effective, the minority carriers should decay with a *theoretical* or radiative lifetime of $1/(BN)$. The latter statement is altered by the strong effects of self-absorption of the photoluminescence. The self-adsorption followed by electron–hole generation and recombination radiation is called *photon recycling*. The photo recycling is significant for GaAs devices with active layers greater than $1.0\,\mu$m thick.

DIAGNOSTIC CONFINEMENT DEVICES

The standard experimental technique revolves around the optical excitation of excess minority carriers (Δp, Δn) by a short pulse of light such as from a pulsed laser. The photoluminescence decays with the excess minority-carrier density as will be shown below. The total PL output is simply given by summing the excess minority carriers over the active volume and multiplying by the radiative probability. The *excess carrier* minority-carrier concentration ρ is the increase in charge density above the equilibrium value. Defining:

$$\rho = \Delta n(p\text{-type}) \quad \text{or} \quad \Delta p(n\text{-type}), \tag{9}$$

the PL intensity is given by:

$$I_{PL}(t) = \frac{1}{\tau_R}\int_V \rho(r, t)\,\mathrm{d}V. \tag{10}$$

We see from eqn (10) that $I_{PL}(t)$ *tracks* $\rho(t)$ in time, which is the basic advantage of TRPL. If $\rho(r, t)$ decays exponentially with the minority carrier lifetime, the PL intensity can be written in terms of the total initial excess density ρ_t:

$$I_{PL}(t) = \frac{\rho_t}{\tau_R}\,\mathrm{e}^{-t/\tau}. \tag{11}$$

If minority carriers diffuse out of the volume (V) to junctions, the PL lifetime is less than the minority-carrier lifetime.

When self-absorption and reflection of the internally generated photon are taken into account, the PL intensity is modified by:

$$I_{PL}(t) = \int_v \frac{A(\bar{r})\rho(\bar{r}, t)\,\mathrm{d}v}{\tau_R}. \tag{12}$$

Here $A(r)$ is an optical interaction function accounting for the self-absorption and interfacial reflection of internally generated photons. For now, I will take $A(r) = 1$.

The excess minority carrier density $\rho(x, t)$ is found by solving the time-dependent diffusion equation:

$$\frac{\partial \rho}{\partial t} = \frac{-\rho}{\tau} + D\,\nabla^2\rho. \tag{13}$$

Integrate $\rho(x, t)$ over the active volume to get the total light output:

$$\frac{\partial}{\partial t}\int_V \rho(\bar{r}, t)\,\mathrm{d}v = -\frac{1}{\tau}\int_V \rho(\bar{r}, t)\,\mathrm{d}v + D\int_V \nabla^2\rho(\bar{r}, t)\,\mathrm{d}v. \tag{14}$$

The last term on the right describes the diffusion of minority carriers in the active volume. One can transform the (right-hand term) Laplacian of ρ to the gradient of J, the particle flux. Using Greens theorem, the volume integral of divergence of J can be transformed to a surface integral over the volume:

$$\int_V \nabla \cdot J\,\mathrm{d}v = \oint_S \bar{J}\cdot\hat{n}\,\mathrm{d}s. \tag{15}$$

The surface integral of J over the surface is the diffusion of minority carriers out of volume V. Thus a *confinement structure* is one in which:

$$\oint_S \bar{J}\cdot\hat{n}\,\mathrm{d}s = 0. \tag{16}$$

Then:

$$\frac{\partial \rho_t}{\partial t} = -\frac{\rho_t}{\tau} \quad \rho_t = \int_V \rho(x, t)\,\mathrm{d} \tag{17}$$

and

$$\rho_t = \rho_t^0 \exp(-t/\tau). \tag{18}$$

This equation shows that the PL decays with the minority-carrier lifetime only when there is no charge flow out of the active region.

A more accurate measurement of minority-carrier lifetime is therefore obtained from a confinement structure which prevents minority-carrier diffusion loss from the active region. A generic confinement structure is shown in Fig. 2. Here one grows a smaller bandgap active region between two wider bandgap layers of like doping type. A simplified schematic of the band structure is superimposed onto Fig. 2. The wide bandgap layers act as minority carrier mirrors.

The first confinement structures[19,20] reported for GaAs were $n^+/n/n^+$ homostructures. These structures are limited, however, to undoped or lightly-doped active layers in order for the confinement barrier to be adequate. The isotype double heterostructure (DH) grown by epitaxy has long been used as a diagnostic confinement device[21–24] for materials in the $Al_xGa_{1-x}As$/GaAs family. The epitaxial growth techniques include metal–organic

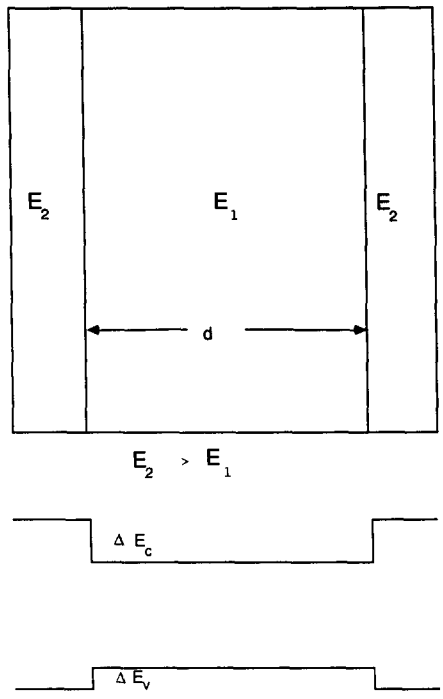

Fig. 2. Schematic of the isotype double heterostructure and the resulting band structure.

chemical vapor deposition (MOCVD), liquid phases epitaxy (LPE) and molecular beam epitaxy (MBE). By measuring the PL lifetime in these relatively simple, contactless devices, one can quickly evaluate the processing technology and predict device performance. For example, one can select the best growth temperature by fabricating these devices over a temperature range. Also for a given growth method, one can evaluate the quality of different source materials by making identical devices using different sources. An example of this type of process development research will be described here.

Transient analysis of the DH structure

A pulsed, monochromatic light source or laser generates electron–hole pairs in the active layer. The transmission of the window layer to the optical excitation wavelength is not usually a limitation as the layer thicknesses is usually kept to several hundred ångstroms. On the other hand, the window thickness must be large enough to prevent minority-carrier tunneling out of the active layer. The preferable wavelength of excitation is chosen so that it is strongly absorbed by the active layer but transmitted by the window layer.

The solution of the 1-D time-dependent diffusion equation [eqn (11)] usually starts with the following substitution:

$$\rho(x, T) \equiv U(x, t)\exp(-t/\tau). \tag{19}$$

Upon substitution into eqn (13), the lifetime terms cancel and the differential equation involving $\rho(x, t)$ is transformed into the well-known equation characteristic of heat flow:

$$\frac{\partial U(x, t)}{\partial t} = D\frac{\partial^2(x, t)}{\partial x^2}. \tag{20}$$

The solutions to the diffusion equation for a variety of geometries and boundary conditions are well-documented in the heat flow literature[25,26]. For the isotype double heterostructure, one uses the solutions of Carslaw and Jaeger for heat flow in thin, infinite planes of thickness d. A trigonometric solution of the general form is assumed with parameters of α_i and b_i determined by boundary conditions:

$$U(x, t) = \sum_i U_i(x, t), \tag{21}$$

where

$$U_i(x, t) = A_i(\cos\alpha_i x + b_i \sin\alpha_i x)\exp(-\beta_i t). \tag{22}$$

Substitution of U into eqn (17) requires term-by-term equality producing the set of relationships:

$$\beta_i = D\alpha_i^2. \tag{23}$$

The boundary conditions at $x = 0$ and $x = d$ equate the diffusion currents and the recombination currents where S is the recombination velocity at both interfaces. For example:

$$\left|qD\frac{\partial U_i}{\partial x} = qU_iS\right|_{x=0}$$

and

$$\left|qD\frac{\partial U_i}{\partial x} = qU_iS\right|_{x=d}. \tag{24}$$

These boundary conditions produce the well-known[27–29] eigenvalue equation for α_i:

$$\tan(\alpha_i d) = \frac{2\dfrac{\alpha_i S}{D}}{\alpha_i^2 - \left(\dfrac{S}{D}\right)^2}. \tag{25}$$

For the case of $S = 0$, the eigenvalues are:

$$\alpha_i = 0, \pi/d, 2\pi/\delta, \ldots$$

$$\beta_i = 0, \pi d^2/D, 4\pi d^2/D, \ldots \tag{26}$$

for $i = 1, 2, 3$, etc. The optical excitation produces an initial excess minority-carrier density according to Beers' law:

$$\rho(x, 0) = I_0\alpha\exp(-\alpha x), \tag{27}$$

where α is the absorption coefficient of the incident monochromatic light. By substitution, one finds A_i to be:

$$A_i = \frac{2\alpha_i^2}{\left[\alpha_i^2 + \left(\dfrac{S}{D}\right)^2\right]d + 2\dfrac{S}{D}} \times \frac{\alpha\left(\alpha + \dfrac{S}{D}\right)}{[\alpha_i^2 + \alpha^2]}. \tag{28}$$

It may be shown that U_i are orthogonal functions over the interval $x = 0$ to d and have the characteristics of eigenfunctions of the differential eqn (20). Finally, one finds $\rho(x, t)$ equal to:

$$\rho(x, t) = \exp(-t/\tau) \sum_{i=1}^{\infty} U_i(x, t). \tag{29}$$

One can integrate eqn (12) above with $A = 1$ and find:

$$I_{PL}(t) = \frac{1}{\tau_R} \sum_{i=1}^{\infty} A_i C_i \exp(-\beta_i t) \exp(-t/\tau). \tag{30}$$

Here C_i comes out of the integration of $U_i(x)$ over the active region using eqn (12). One can now easily include the 1-D self-absorption by including the absorption coefficient β of the radiation that is being passed by the spectrometer. Then $A(r)$ is equal to $\exp(-\beta x)$ in this approximation and:

$$I_{PL}(t) = \frac{1}{\tau_R} \int_0^d \rho(x, t) \exp(-\beta x)\, dx. \tag{31}$$

By evaluation of the somewhat laborious algebra, it may be shown:

$$C_i = \frac{\beta + S/D}{\beta^2 + \alpha_i^2} - \frac{\exp(-\beta d)}{\beta^2 + \alpha_i^2} \left\{ (\beta + S/D)\cos(\alpha_i d) + \left(\frac{S\beta}{\alpha_i D} - \alpha_i \right) \sin(\alpha_i d) \right\}. \tag{32}$$

For observation times which are long compared to characteristic diffusion times corresponding to $\beta_2 (> \pi d^2/D)$ in eqn (23), the first term of the Fourier expansion ($\beta_1 \sim 2S/d$) dominates the time decay. From eqn (30), one finds an effective lifetime:

$$\frac{1}{\tau_{PL}} = \frac{1}{\tau_B} + \frac{2S}{d}, \tag{33}$$

where S is the interface recombination velocity at each heterointerface. By making two structures which are identical except for the active-layer thickness d, one can obtain unique values of bulk lifetime and S. If the DH device is fabricated of the same materials as proposed for the working device, one measures the bulk lifetime and S for the latter. This information is useful for device design and modelling.

Photon recycling

The self-absorption and reemission of radiative recombination was proposed by workers[30] several years before an experimental observation was made. Early experimental work[31] on TRPL in $Al_xGa_{1-x}As$/GaAs DH devices showed that the lifetime increased with active layer thickness. In this work, the data indicated lifetimes which were five times larger than the calculated radiative lifetime of 4.1 ns at $N = 1.2 \times 10^{18}\,cm^{-3}$ in a ($d = 10\,\mu m$) DH device. Later calculations by Asbeck[32], Garbuzov[33] and coworkers and others[34,35] used the photon recycling model to explain why $\tau_{PL} > \tau_R$. According to these calculations, the bulk lifetime of a DH device can be written in terms of a photon recycling factor $\phi(d)$ as:

$$\frac{1}{\tau_B} = \frac{1}{\tau_{nR}} + \frac{1}{\phi \tau_R}, \tag{34}$$

where τ_B is the bulk minority carrier lifetime. The photoluminescence lifetime of a DH structure can then be written as:

$$\frac{1}{\tau_{PL}} = \frac{1}{\tau_{nR}} + \frac{1}{\phi \tau_R} + \frac{2S}{d} = \frac{1}{\tau_{nR}} + \frac{1}{\phi \tau_R} + \frac{1}{\tau_S}. \tag{35}$$

Here one can replace $d/2S$ by τ_S, the surface lifetime.

The Asbeck calculations of $\phi(d)$ for DH structures with different doping levels and $Al_xGa_{1-x}As$ window layer compositions are shown in Fig. 3. The recycling factor $\phi(d)$, calculated for an AlGaAs/GaAs DH structure, increases almost linearly with the active layer thickness d. One sees that ϕ is greater than 10 for undoped GaAs active layers with a 10 μm thickness. A later section will give a number of experimental results confirming the size of the photon recycling effect.

EXPERIMENTAL RESULTS

Undoped GaAs/$Al_xGa_{1-x}As$ diagnostic structures

A useful technique to evaluate the SRH bulk and interface recombination in a particular epitaxial growth reactor is to fabricate an undoped $Al_xGa_{1-x}As$/GaAs DH structure. The radiative recombination rate (BN where N is the background doping) in undoped services is usually much less than the SRH recombination rate (i.e. $\phi\tau_R \gg \tau_{SRH}$). In other words, except for exceptionally defect-free material, the SRH process will be dominant in undoped GaAs. The $\phi\tau_R$ term in eqn (35) is then much larger than the surface lifetime ($2d/S$ and/or the bulk SRH lifetime. From eqn (35) above, one sees that the bulk SRH and the interface S control the PL lifetime in this case. If the active layer thickness d is made

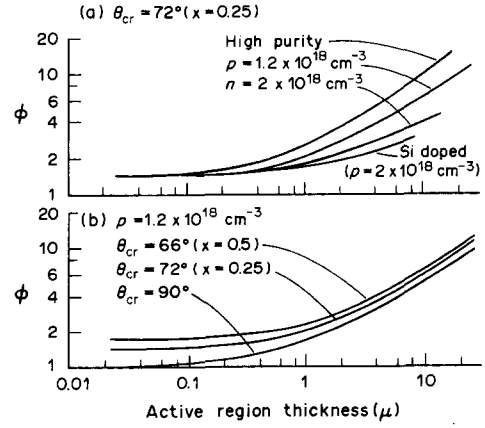

Fig. 3. The calculations of Asbeck for photon recycling in a DH structure from Ref. [27].

sufficiently small, the surface lifetime ($2d/S \ll \tau_{SRH}$) will dominate the total PL lifetime. Then:

$$\frac{1}{\tau_{PL}} = \frac{2S}{d}. \tag{36}$$

Nelson and Sobers[24] fabricated an undoped ($p = 1.9 \times 10^{15}\,cm^{-3}$) DH structure with $d = 16\,\mu m$ by LPE. The TRPL lifetime of this device was 1.3 μs, which was far larger than any previously measured GaAs lifetime. With a photon recycling factor greater than 10 and τ_R of about 5 μs, they assumed that the lifetime of this device is SRH limited. The maximum value of S is 615 cm s^{-1} if one assumes that the surface lifetime dominates. An unambiguous breakdown into bulk SRH and S could be made if two devices were measured, which are identical except for d.

Since this early work, numerous workers have found lifetimes greater than 1 μs in undoped, GaAs DH structures. The TRPL lifetime[36], of a typical, undoped MOCVD $Al_xGa_{1-x}As$/GaAs device grown at SERI is shown in Fig. 4. The active layer thickness d is 1.8 μm and the TRPL lifetime is 1.1 μs. Assuming the surface lifetime dominates the TRPL according to eqn (36), one calculates $S = 82$ cm s^{-1}. In any case, this again represents the maximum value of S. Dawson and Woodbridge[37] found that buffer or prelayers grown between the substrate and the DH device reduced S below 100 cm s^{-1} for their structures grown by MBE. They measured a PL lifetime of 125 ns in a structure with $d = 0.2\,\mu m$. This corresponds to $S \sim 80$ cm s^{-1} using eqn (33). For devices without prelayers, S was found to be 4×10^3–6×10^3 cm s^{-1}. The work of Yablonovitch[38] and coworkers also indicated that similar (approx. 1 μs) lifetimes were found in $Al_xGa_{1-x}As$/GaAs DH structures grown by LPE, MOCVD and MBE of unspecified thicknesses. A number of other workers[39, 40] report lifetimes in the ~ 1 μs range for d in the range 5–10 μm. The report of Smith and coworkers described an $n^+/n/n^+$ diagnostic structure with an 8 μm active layer.

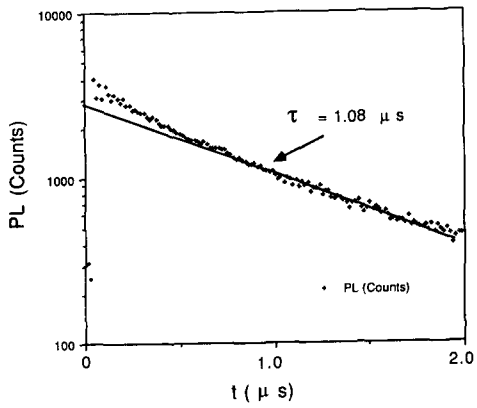

Fig. 4. The time-resolved photoluminescence of a 1.8-μm-thick, undoped GaAs DH device at 300 K.

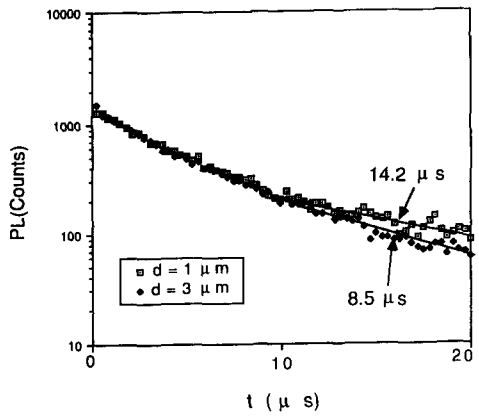

Fig. 5. The time-resolved photoluminescence of two undoped GaInP/GaAS DH structures at 300 K.

A classic example of TRPL complementing process research was demonstrated by Molenkamp *et al.*[41]. This work examined the PL lifetime in undoped, 4.0 μm $Al_xGa_{1-x}As$/GaAs DH structures as a function of the arsine pressure during MOCVD growth. They found a steep lifetime maximum of 4.9 μs in a device grown at 15×10^{-4} atm of arsine pressure.

Other studies have coordinated the PL lifetime measurement with substrate orientation, grown materials obtained from different vendors, arsine purification, III/V ratio[42], etc. The ease of making the DH diagnostic devices combined with the simplicity of the TRPL measurement allow such experimentation with process and materials research.

Undoped GaAs/GaInP diagnostic structures

The ternary $Ga_{0.5}In_{0.5}P$ is lattice-matched to GaAs and has a bandgap from 1.8 to 1.9 eV depending upon growth conditions. $Ga_{0.5}In_{0.5}P$ has been found to be an effective window/passivating layer for GaAs. Figure 5 shows the TRPL data for two undoped GaAs/GaInP DH structures with GaAs layer thicknesses of 1.0 μm (A) and 3.0 μm (B). The residual doping in the GaAs active layers is n-type 2–5×10^{14} cm^{-3}. The PL decay is bimolecular[5,38] (and nonexponential) in the initial portion of the decay as the structure is excited into high injection. After some time, the decay becomes exponential indicating low injection conditions prevail. The low injection lifetime has, of course, been the subject of the previous derivations. The 1.0 μm device has a PL lifetime[43] of 14.2 μs, which is the *largest lifetime* ever reported for GaAs. Using eqn (36), the calculated S is 3.5 cm s^{-1}. However, the PL lifetime was measured as a function of temperature (T) from 77 to 300 K and found to vary as $T^{1.59}$. The radiative lifetime[44] varies as $T^{1.5}$ and is therefore an appreciable component of the total PL lifetime here. The PL lifetime is then given by:

$$\frac{1}{\tau_{PL}} = \frac{1}{\phi\tau_R} + \frac{2S}{d}, \tag{37}$$

where $\phi \sim 1$ for the 1.0 device. Assuming that the residual doping is $2 \times 10^{14}\,cm^{-3}$ ($5 \times 10^{14}\,cm^{-3}$), one calculates $S = 2.6\,cm\,s^{-1}$ ($1.1\,cm\,s^{-1}$). These are then significantly smaller than any reported S-values for the $Al_xGa_{1-x}As/GaAs$ interface.

Doping dependence of S

The S-values which are measured for either undoped $Al_xGa_{1-x}As/GaAs$ or undoped GaInP/GaAs DH structures are much smaller than those reported for more heavily doped devices. The physics here indicate that the band-bending, if repulsive for minority carriers, reduces the excess concentration at the interfaces and thereby reduces the effective S. In this sense, the values of S which are reported in the above sections are not representative of those found at more common device levels, i.e. $N \sim 10^{17}$–$10^{19}\,cm^{-3}$. In the following section, I will show that the minimum S found at $N_D \sim 10^{17}\,cm^{-3}$ is about $500\,cm\,s^{-1}$ as compared with $S < 100\,cm\,s^{-1}$ for the above undoped devices. Recent work[45] using GaInP as a window layer for moderately-doped GaAs ($N = 1.5 \times 10^{17}\,cm^{-3}$) reported minimum S-values of $200\,cm\,s^{-1}$ compared with $2\,cm\,s^{-1}$ for the undoped structures. As undoped GaAs has relatively few device applications, these studies are more indicative of the health of the growth apparatus. For device modelling purposes, the diagnostic device should have a comparable doping level to the real device.

Minimization of S at the doped GaAs/$Al_xGa_{1-x}As$ interface

Here I will illustrate another example of materials research using complementary time-resolved PL measurements. These measurements[46,47] were done in collaboration with workers at the Spire Corporation with the goal of maximizing the performance of a single-junction GaAs solar cell. These devices were MOCVD grown single-junction devices using $Al_xGa_{1-x}As$ passivation layers on the GaAs p–n junction. The choice of growth temperature was complemented by TRPL measurments on double heterostructures which were doped n-type to 1–$2 \times 10^{17}\,cm^{-3}$ and p-type to $2 \times 10^{18}\,cm^{-3}$. The diagnostic DH devices simulated the n-base and p-emitter regions of the solar cell, respectively, and produced values of the minority carrier lifetime and interface recombination velocity. At each growth temperature, several DH diagnostic devices were grown with active layer thickness d varying over the range from about 1, 2, 4 and 8 μm. The Al composition of the $Al_xGa_{1-x}As$ window layers was $x = 0.30$. Figure 6 shows the variation of heterointerface recombination velocity S and the ratio of τ_{PL}/τ_R with growth temperature for 4-μm devices. The experimental analysis included the photon recycling effect as $\tau_{PL} \ll \tau_R$ for growth temperatures greater than 740°C. Equation (37) was used in this analysis, including a value of ϕ which was calculated[48]

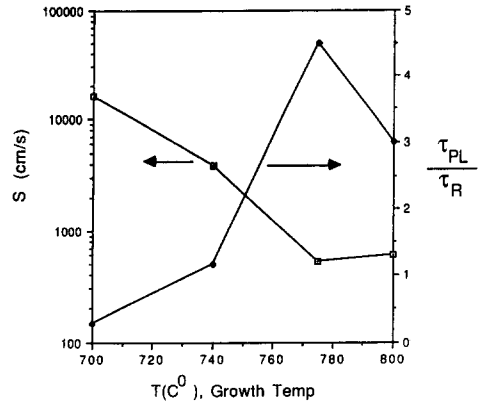

Fig. 6. The interface recombination velocity and ratio of PL lifetime divided radiative lifetime vs growth temperature. The thickness of the DH devices is 4.0 μm and the doping levels are 1–$1.5 \times 10^{17}\,cm^{-3}$.

specifically for these devices. The interface recombination velocity was found to vary from a minimum of about $500\,cm\,s^{-1}$ at 775°C growth temperature to $20{,}000\,cm\,s^{-1}$ at 700°C. The 775°C growth temperatures were then used to fabricate the photovoltaic devices. A single-junction photovoltaic device, which was grown under these conditions, has a one sun efficiency[49] to 24.8%. This was the largest reported efficiency for a single-junction device at the time.

Photon recycling in n-GaAs

The previous section indicated that PL lifetimes greatly exceeded the radiative lifetime in DH devices grown about 740°C. To explain the data by inaccuracy in the B-coefficient requires B-values 5–10 times smaller than the accepted value. The B-coefficient is fairly well-established by both calculation[50] and experiment[51]. Van Roosbroeck and Shockley derived a relationship[52] between the B-coefficient and the integrated absorption spectrum using detailed balance. Application[14] of this relationship to GaAs indicates that the calculated B is consistent with the absorption data. If the B-coefficient is correct, this data implies that photon recycling must account for this discrepancy. Recent TRPL work[53] on angle-lapped DH devices indicated that the lifetime increased as the excitation point was scanned to thicker portions of the active layer. This work included calculations of the photon recycling factor on the TRPL and these agreed quite well with the data.

The work[47] above measured lifetimes in DH structures which exceeded the radiative lifetime by factors of 3–8 in devices with active layers of 4–8 μm width. The majority-carrier electron concentrations were accurately measured with a Polaron profiler and were in the range 1×10^{17}–$1.5 \times 10^{17}\,cm^{-3}$ n-type. Using $B = 2 \times 10^{-10}\,cm^3\,s^{-1}$. the radiative lifetime range τ_R is 50–33 ns, respectively. Figure 7 shows TRPL data on an 8 μm device with $N = 1.3 \times 10^{17}\,cm^{-3}$ which was grown at 775°C. The ultra-long lifetime must be attributed to photon recycling.

Calculations[54] of $\phi(d)$ on these specific structures were done by the group at the University of Colorado and agree quite well with the data. The measured PL lifetime of 290 ns is more than 7.5 times the radiative lifetime. As expected from theory, the PL lifetime approached the radiative lifetime as d was made smaller. The analysis of the 775°C grown structures of different thickness d was consistent with a constant interface recombination velocity (about 500 cm s^{-1}) and Miller's calculated[47] $\phi(d)$. In other words, one can only fit eqn (37) to the data sets with a constant S if the recycling factor $\phi(d)$ is included in the fit.

The photon recycling effects must be considered in device design and modeling and may be utilized to improve device performance. Partain *et al.* [55] measured the spectral response and diffusion length in heavily-doped GaAs homojunctions. This work indicated diffusion lengths that were longer than a "theoretical" maximum obtained from the majority carrier diffusivity and τ_R. These devices had quantum efficiencies exceeding the "theoretical" maximum. The explanation offered in that work is that photon recycling increases the lifetime above the theoretical limit producing an enhanced diffusion length. Other experimental evidence has suggested that photon recycling is a significant effect in GaAs photovoltaic devices. A recycling effect was recently designed into a GaAs single quantum well laser structure[56] and reduced the laser threshold current by a factor of two. The active region self-absorption is quite small in a quantum well device. The device utilized an epitaxially grown photodiode to convert the spontaneous radiation from the laser into pump current. This configuration is novel in that the external spontaneous radiation was collected and recycled.

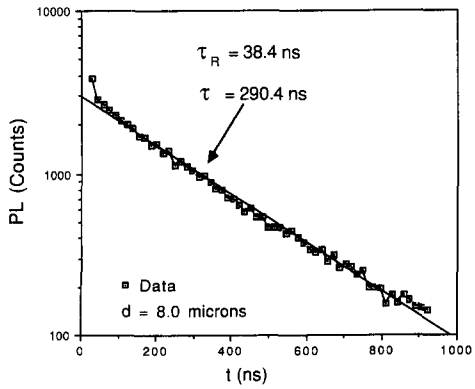

Fig. 7. DH structure with active layer thickness of 8.0 μm and active layer doping level of 1.3×10^{17} cm^{-3}. The device was grown at 775°C.

Intensity dependence of SRH lifetime

The minority-carrier lifetime in Si is usually controlled by SRH recombination and has been shown[57] to be dependent upon the injection level of excess carriers. Recent work[58,59] has shown similar effects in the III–V compound semiconductors. The net effect is that a single lifetime does not exist but the recombination rate changes continuously with the injection level. Here I will analyze the effect of SRH recombination on the TRPL measurement. The model case of an n-type semiconductor (carrier density N_D) and excess injected carrier density Δp, Δn ($\Delta p = \Delta n$) will be analyzed. The SRH recombination rate of eqn (3) becomes:

$$\frac{d\,\Delta p}{dt} = -\frac{\sigma_n \sigma_p v_{th} N_t [\Delta p N_D - \Delta p^2]}{\sigma_n [N_D + \Delta p + n_i \exp(E_t - E_i/kT) + \sigma_p [\Delta p + n_i \exp(E_i - E_t/kT)}. \tag{38}$$

Here v_{th} is the hole thermal velocity, N_t is the defect density cm^{-3} and $\sigma_n(\sigma_p)$ are the capture cross-sections for electrons (holes), respectively. Dividing by the right-hand side of eqn (35) by $\sigma_n \sigma_p v_{th} N$ and using the definitions of electron and hole lifetime:

$$\frac{t}{\tau_n} = \frac{1}{v_{th} N \sigma_n},$$
$$\frac{1}{\tau_p} = \frac{1}{v_{th} N \sigma_p}. \tag{39}$$

This equation becomes:

$$\frac{d\Delta p}{dt} = -\frac{\Delta p N_D + \Delta p^2}{\tau_p [N_D + \Delta p] + \tau_n \Delta p}. \tag{40}$$

Defining the excess carrier density by $I(t)$ which is the instantaneous injection level:

$$I(t) \equiv \frac{\Delta p(t)}{N_D}. \tag{41}$$

Eqn (37) then becomes:

$$\frac{dI}{dt} = -\frac{I + I^2}{\tau_p [1 + I] + \tau_n I}. \tag{42}$$

The solutions of eqn (6) are:

$$I(t) = \exp(-t/\tau_p), \qquad (I \ll 1),$$
$$I(t) = \exp[-t/(\tau_p + \tau_n)], \quad (I \gg 1). \tag{43}$$

Figure 8 shows the PL decay of an n-type $Al_xGa_{1-x}As$/GaAs DH device with N_D equal to 1.5×10^{17} cm^{-3} and the active layer thickness $d = 8.0$ μm. The n-type DH structure was grown at the Spire Corporation at 700°C and is a data point of Fig. 6. The decay rate is nonexponential over an appreciable range of excess hole densities. One can fit the initial decay ($0 < t < 50$ ns) with a lifetime of 63.5 ns. The decay from 50 to about 200 ns is nonexponential and cannot be described by a single lifetime. At longer times (about 200–300 ns), the data

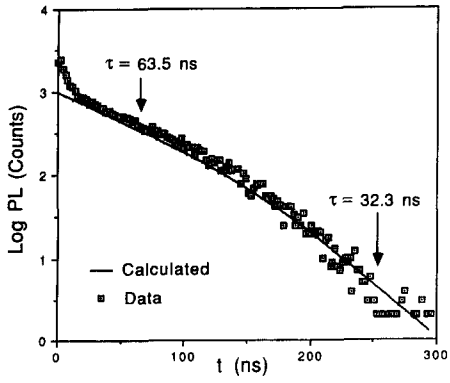

Fig. 8. The time-resolved photoluminescence of a 8.0 μm DH device grown at 700°C. The doping level is $1.5 \times 10^{17}\,cm^{-3}$ n-type.

can be described with an effective lifetime of 32.3 ns. The calculated radiative lifetime for this doping level is 33.3 ns and the photon recycling factor is greater than 10 in an 8 μm DH device. Therefore the effective radiative lifetime is over 330 ns and not controlling the lifetime here. The shorter lifetime measured here is therefore controlled by nonradiative SRH recombination. Equation (39) was integrated by the Runge–Kutta technique[60] using a minority carrier lifetime of 32.3 ns and a majority carrier lifetime of 31.2 ns and an initial injection ratio of 20. This I-value was used as it is consistent with calculations using the incident laser energy density and Beer's law absorption. The results of the numerical integration are shown as the solid line in the figure.

The characteristic downturn of the decay curve has been seen in numerous devices and is an indicator of dominant SRH recombination. Other work has shown that one may separate bulk and interface recombination by the appropriate experiments. When interface recombination is the dominant mechanism, the TRPL may be fit with a function of the form:

$$\frac{dI}{dt} = -\frac{I + I^2}{\tau_{sp}[1 + I] + \tau_{sn} I}. \tag{44}$$

Here the surface lifetimes for holes and electrons are respectively:

$$\tau_{sp} = \frac{d}{2S_p},$$
$$\tau_{sn} = \frac{d}{2S_n}. \tag{45}$$

The quantities S_p and S_n are interface recombination velocities for holes and electrons, respectively. By varying the active layer thickness d, one can determine if the dominant recombination mechanism is bulk or surface related. The work here on devices grown at 770°C was indicative of interface recombination controlling the minority-carrier lifetime.

Dislocation recombination: GaAs grown on silicon

There have been many reports[61] of GaAs majority carrier devices grown upon an Si substrate. A difficulty associated with the GaAs/Si system is the 4% lattice mismatch which results in the generation of dislocation densities exceeding $10^8\,cm^2$ in the GaAs. This is an ideal system for studying the SRH recombination process at dislocations. In the studies to be described here, isotype DH structures of n-$Al_xGa_{1-x}As$/GaAs are grown on Si substrates. Recent studies[62] indicate that the minority carrier lifetime is reduced three or four orders of magnitude by recombination at dislocations. The dislocation density is reduced by special buffer layer grown between the GaAs active region and the substrate[63, 64]. The DH diagnostic device is then grown on top of the strain-reduction layers. The data of Fig. 9 are for two devices (B and C) that were grown on Si substrates. The buffer layer is 8 μm thick for the GaAs/Si devices B and C. DH Structures which were grown directly on Si typically produced minority-carrier lifetimes in the picosecond range. Device A is a control device grown of GaAs and the dislocation density is in the range of $1 \times 10^4\,cm^{-2}$. Device B has an unannealed 8 μm buffer layer and device C has an 8 μm thermally annealed buffer layer. The degradation of lifetime with dislocation density is obvious from the figure. The measured lifetime here is 0.82 ns for device B and 1.79 ns for device C of Fig. 9. Saturation of these defects was weak to unobservable at the dislocation levels in these samples.

A model of the recombination rate at dislocations has been derived by Yamaguchi *et al.*[65] and the latter is added to eqn (34):

$$\frac{1}{\tau_{PL}} = \frac{1}{\phi\tau_R} + \frac{2S}{d} + \frac{\pi^3 D N_d}{4}. \tag{46}$$

Here N_d is the average density of dislocations (cm^{-2}) and D is the minority-carrier diffusivity. The lifetime vs dislocation density N_d for 14 GaAs/Si devices is plotted in Fig. 10. The model replaces the radiative

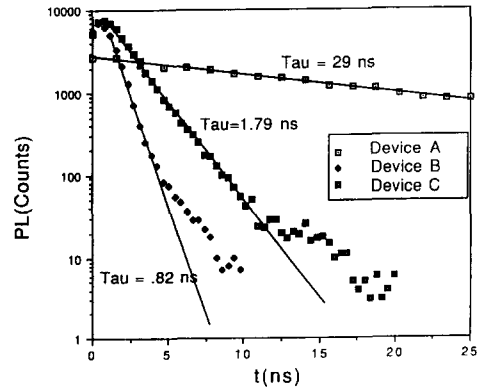

Fig. 9. The time-resolved photoluminescence of three n-type $Al_xGa_{1-x}As$/GaAs DH structures with a 4.0 μm active layer thickness and doping level of about $1 \times 10^{17}\,cm^{-3}$. Device A: grown on a GaAs substrate. Devices B and C: grown on an Si substrate with GaAs buffer layers. The buffer layers are B (unannealed) and C (thermally annealed).

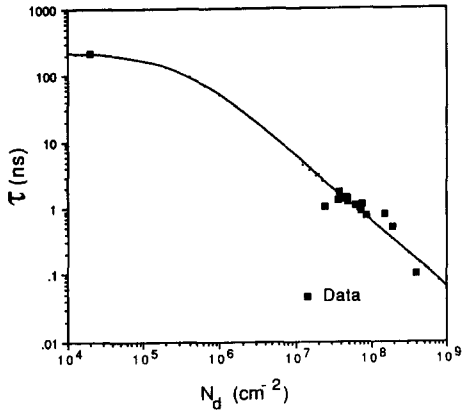

Fig. 10. Composite data lifetime of $Al_xGa_{1-x}As$/GaAs DH structures grown on Si vs dislocation density.

and surface recombination terms with a control device lifetime of 30 ns and the diffusivity was chosen as $2\,cm^2\,s^{-1}$. The model predicts the minority carrier lifetime very well for dislocation densities greater than about $5 \times 10^7\,cm^{-2}$ as can be seen from the figure. The model predicts that N_d must be reduced below $10^6\,cm^{-2}$ in order to avoid dislocation-limited lifetimes. To this authors knowledge, dislocation densities below $10^6\,cm^{-2}$ have not been reported for GaAs grown on Si.

SUMMARY

The time-resolved photoluminescence (TRPL) has been demonstrated to be a powerful characterization tool for process development of minority-carrier devices. One of the examples here indicated that the optimum MOCVD growth temperature can be determined by making simple DH diagnostic devices with the same components as the desired, more complicated device. The TRPL measurement is the qualifying diagnostic tool in choosing the best growth temperature. Other work has described a similar procedure in qualifying source materials, as for example, arsine in an MOCVD reactor. Also described here are measurements used to compare the passivating window layers in $Al_xGa_{1-x}As$/GaAs and GaInP/GaAs heterojunction devices. The photon recycling effect becomes very important as SRH recombination is reduced and active layer thickness increases. Lattice-mismatched systems such as GaAs grown on Si have devastating reductions of the minority-carrier lifetime. The dominance of SRH recombination may be discerned by an intensity-dependent lifetime which changes with the excess minority-carrier density at high injection levels.

Acknowledgements—The author wish to thank A. Nozik, S. M. Vernon and J. Olson for providing the samples and devices used in these studies. I also wish to thank M. M. Al-Jassim for the TEM dislocation studies of the GaAs/Si system. I finally wish to thank colleagues D. J. Dunlavy, B. M. Keyes and D. Levi for providing the profuse TRPL data which was the basis for this publication.

REFERENCES

1. D. K. Schroder, *Semiconductor Material and Device Characterization*, pp. 359–447. Wiley, New York (1990).
2. J. W. Orton and P. Blood, *The Electrical Characterization of Semiconductors: Measurement of Minority-carrier measurements Properties*, pp. 51–122. Academic Press, London (1990).
3. R. K. Ahrenkiel, D. J. Dunlavy and M. L. Timmons, *Twentieth IEEE Photovoltaics Specialists Conf.*, p. 611 (1988).
4. R. K. Ahrenkiel, *Memorias VIII Congreso Nacional de Fisica de Superficies E Interfaces*, p. 1 (1988).
5. R. K. Ahrenkiel, *Current Topics in Photovoltaics*, Vol. 3, pp. 1–75. Academic Press, London (1988).
6. R. K. Ahrenkiel, D. J. Dunlavy and H. C. Hamaker, *Solar Cells* **21**, 353 (1987).
7. R. Z. Bachrach, *Rev. Sci. Instr.* **43**, 734 (1972).
8. R. K. Ahrenkiel, D. J. Dunlavy and T. Hanak, *Solar Cells* **24**, 339 (1988).
9. W. Shockley and W. T. Read, *Phys. Rev.* **87**, 335 (1952).
10. R. N. Hall, *Phys. Rev.* **87**, 387 (1952).
11. C. T. Sah, R. N. Noyce and W. Shockley, *Proc. IRE* **45**, 1228 (1957).
12. R. N. Hall, *Proc. Inst. Elect. Engng* **106B** (Suppl. 17), 983 (1960).
13. F. Stern, *J. appl. Phys.* **47**, 5382 (1976).
14. H. C. Casey Jr and F. Stern, *J. appl. Phys.* **47**, 631 (1976).
15. S. M. Sze, *Physics of Semiconductor Devices*. Wiley, New York (1981).
16. J. I. Pankove, *Optical Processes in Semiconductors*. Dover, New York (1971).
17. C. J. Hwang, *J. appl. Phys.* **43**, 4408 (1971).
18. M. S. Lundstrom, M. E. Klausmeier-Brown, M. R. Melloch, R. K. Ahrenkiel and B. M. Keyes, *Solid-St. Electron.* **33**, 693 (1990).
19. P. D. Dapkus, N. Holonyak Jr, R. D. Burnham and D. L. Keune, *Appl. Phys. Lett.* **16**, 93 (1970).
20. P. D. Dapkus, N. Holonyak Jr, R. D. Burnham, D. L. Keune, J. W. Burd, K. L. Lawley and R. E. Walline, *J. appl. Phys.* **41**, 4194 (1979).
21. D. L. Keune, N. Holonyak Jr, R. D. Burnham, D. R. Scifres, H. W. Zwicker, J. W. Burd, M. G. Craford, D. L. Dickus and M. J. Fox, *J. appl. Phys.* **42**, 2048 (1971).
22. R. J. Nelson, *J. Vac. Sci. Technol.* **15**, 1475 (1978).
23. R. J. Nelson and R. G. Sobers, *Appl. Phys. Lett.* **32**, 761 (1978).
24. R. J. Nelson and R. G. Sobers, *J. appl. Phys.* **49**, 6103 (1978).
25. H. S. Carslaw and J. C. Jaeger, *Conduction of Heat in Solids*, 2nd Edn. Oxford University Press (1978).
26. J. Crank, *The Mathematics of Diffusion*, 2nd Edn. Clarendon, Oxford (1975).
27. See Ref. [25], p. 115.
28. M. Boulou and D. Bois, *J. appl. Phys.* **48**, 4713 (1977).
29. R. K. Ahrenkiel and D. J. Dunlavy, *J. Vac. Sci. Technol.* **A7**, 822 (1989).
30. F. Stern and J. M. Woodall, *J. appl. Phys.* **45**, 3904 (1974).
31. M. Ettenberg and H. Kressel, *J. appl. Phys.* **47**, 1538 (1976).
32. P. Asbeck, *J. appl. Phys.* **48**, 820 (1977).
33. D. Z. Garbuzov, A. N. Ermakova, V. D. Rumyanstev, M. K. Trukan and V. B. Khalfin, *Sov. Phys. Semicond.* **11**, 419 (1977).
34. T. Kuriyama, T. Kamiya and H. Yanai, *Jap. J. appl. Phys.* **16**, 465 (1977).
35. T. Kamiya, S. Hirose and H. Yanai, *J. Luminesc.* **18**, 910 (1979).
36. A. Nozik and R. K. Ahrenkiel, Unpublished data (1988).

37. P. Dawson and K. Woodbridge, *Appl. Phys. Lett.* **45,** 1227 (1984).
38. E. Yablonovitch, R. Bhat, J. P. Harbison and R. A. Logan, *Appl. Phys. Lett.* **50,** 1197 (1987).
39. G. W. 't Hooft, M. R. Leys and F. Roozeboom, *Jpn. J. appl. Phys.* **24,** L761 (1985).
40. L. M. Smith, D. J. Wolford, J. Martinsen, R. Venkatasubramanian and S. K. Ghandhi, *J. Vac. Sci. Technol.* **B8,** 787 (1990).
41. L. W. Molenkamp, G. L. M. Kampschoer, W. de Lange, J. W. F. M. Maes and P. J. Roksnoer, *Appl. Phys. Lett.* **54,** 1992 (1989).
42. M. L. Timmons, J. A. Hutchby, R. K. Ahrenkiel and D. J. Dunlavy, *Inst. Phys. Conf. Ser. No. 96*, p. 289 (1989).
43. J. M. Olson, R. K. Ahrenkiel, D. J. Dunlavy, B. M. Keyes and A. E. Kibbler, *Appl. Phys. Lett.* **55,** 1208 (1989).
44. H. Karamon, T. Masumot and Y. Makino, *J. appl. Phys.* **57,** 3527 (1985).
45. R. K. Ahrenkiel, J. M. Olson, D. J. Dunlavy, B. M. Keyes and A. E. Kibbler, *J. Vac. Sci. Technol.* **A8,** 3002 (1990).
46. R. K. Ahrenkiel, D. J. Dunlavy, B. M. Keyes, S. M. Vernon, S. P. Tobin and T. M. Dixon, *21st IEEE Photovoltaics Specialists Conf.*, p. 432 (1990).
47. R. K. Ahrenkiel, D. J. Dunlavy, B. M. Keyes, S. M. Vernon, T. M. Dixon, S. P. Tobin, K. L. Miller and R. E. Hayes, *Appl. Phys. Lett.* **55,** 1088 (1989).
48. K. L. Miller, University of Colorado at Boulder, M.S.E.E. Thesis (1989).
49. S. P. Tobin, S. M. Vernon, C. Bajgar, S. J. Wojtczuk, M. R. Melloch, A. Keshavarzi, T. B. Stellway, S. Venkatensan, M. S. Lundstrom and K. A. Emery, *IEEE Trans. Electron Devices* **37,** 469 (1990).
50. H. C. Casey, Private Communication.
51. G. W. t Hooft, *Appl. Phys. Lett.* **39,** 389 (1981).
52. W. Van Roosbroeck and W. Shockley, *Phys. Rev.* **94,** 1558 (1954).
53. B. Bensaid, F. Raymond, M. Lerous, C. Verie and B. Fofana, *J. appl. Phys.* **66,** 5542 (1989).
54. K. L. Miller, University of Colorado at Boulder, M.S.E.E. Thesis (1989).
55. L. D. Partain, D. D. Liu, M. S. Kuryla, R. K. Ahrenkiel and S. E. Asher, *Solar Cells* **28,** 223 (1990).
56. Y. Gigase, C. S. Harder, M. P. Kesler, H. P. Meier and B. Van Zeghbroeck, *Appl. Phys. Lett.* **57,** 1310 (1990).
57. *Properties of Silicon, EMIS Datareviews Series No. 4*, p. 167 INSPEC, The Institution of Electrical Engineers, London (1988).
58. R. K. Ahrenkiel, B. M. Keyes and D. J. Dunlavy, *J. appl. Phys.* **70,** 225 (1991).
59. M. L. Timmons, T. S. Colpitts, R. Venkatasubramaiian, B. M. Keyes, D. J. Dunlavy and R. K. Ahrenkiel, *Appl. Phys. Lett.* **56,** 1850 (1990).
60. W. H. Press, B. P. Flanner, S. A. Teukolsky and W. T. Vetterling, *Numerical Recipes*, p. 550. Cambridge University Press (1986).
61. *Heteroepitaxy on Silicon*: *Fundamentals, Structure, and Devices* (Edited by H. K. Choi, R. Hull, H. Ishiwara and R. J. Nemanich), *Mater. Res. Soc. Symp. Proc.* Vol. 116, Reno, NV, pp. 179–282 (1989).
62. R. K. Ahrenkiel, M. M. Al-Jassim, D. J. Dunlavy, K. M. Jones, S. M. Vernon, S. P. Tobin and V. E. Haven, *Appl. Phys. Lett.* **53,** 222 (1988).
63. S. M. Vernon, R. K. Ahrenkiel, M. M. Al-Jassim, T. M. Dixon, K. M. Jones, S. P. Tobin and N. H. Karam, *Mater. Res. Soc. Symp. Proc.* (1989).
64. R. K. Ahrenkiel, M. Al-Jassim, D. J. Dunlavy, K. M. Jones, S. M. Vernon, S. P. Tobin and V. E. Haven, *Twentieth IEEE Photovoltaics Specialists Conf.* (1988).
65. M. Yamaguchi, A. Yamamoto and Y. Itho, *J. appl. Phys.* **59,** 1751 (1986).